

NANO EXPRESS

Open Access

Ion beam-induced shaping of Ni nanoparticles embedded in a silica matrix: from spherical to prolate shape

Hardeep Kumar^{1*}, Santanu Ghosh¹, Devesh Kumar Avasthi², Debdulal Kabiraj², Arndt Mücklich³, Shengqiang Zhou³, Heidemarie Schmidt³, Jean-Paul Stoquert⁴

Abstract

Present work reports the elongation of spherical Ni nanoparticles (NPs) parallel to each other, due to bombardment with 120 MeV Au⁺⁹ ions at a fluence of 5×10^{13} ions/cm². The Ni NPs embedded in silica matrix have been prepared by atom beam sputtering technique and subsequent annealing. The elongation of Ni NPs due to interaction with Au⁺⁹ ions as investigated by cross-sectional transmission electron microscopy (TEM) shows a strong dependence on initial Ni particle size and is explained on the basis of thermal spike model. Irradiation induces a change from single crystalline nature of spherical particles to polycrystalline nature of elongated particles. Magnetization measurements indicate that changes in coercivity (H_c) and remanence ratio (M_r/M_s) are stronger in the ion beam direction due to the preferential easy axis of elongated particles in the beam direction.

Introduction

Metal nanoparticles (NPs) embedded in transparent matrices are the subject of large scientific and technological interest as they show significantly different properties as compared to their bulk counterpart [1,2]. The NP size and shape, orientation, interparticle separation and dielectric constant of the surrounding matrix are the crucial parameters which control their properties. Generally, the NP shape and orientation is difficult to control by synthesis parameters. One of the interesting aspects of shape anisotropy in noble metal NPs is the splitting of the surface plasmon resonance band [3-6], which can be tuned from visible to infrared region. Prolate-shaped NPs/nanorods show new and improved photonic, optoelectronic, and sensing properties as compared to spherical NPs [3,5]. On the other hand, an array of magnetic prolate-shaped NPs/nanorods with perpendicular magnetic anisotropy permits to overcome the problem of superparamagnetic instability arising due to the decrease in the particle size in magnetic recording media [6-8]. Another requirement for recording at high

density with a minimum noise is to reduce the interaction between magnetic nanorods, which can be achieved by encapsulation of magnetic nanorods in a non-magnetic matrix. In literature, various methods are reported to prepare prolate-shaped NPs/nanorods, but the investigated methods yield randomly oriented structures (e.g., by chemical routes) [3], small areas (e.g., by electron or focused ion-beam lithography) [5,7] or are limited to a specific class of materials (e.g., porous alumina template growth) [6,8].

Swift heavy ion (SHI) irradiation is an important tool in the modification of materials and is extensively used to manipulate the matter at nanometer scale. One of the important effects of SHI irradiation is the anisotropic shape deformation of amorphous silica nanospheres to oblate shape [9,10] and crystalline metallic NPs, e.g., Co [11,12], Au [13-17], Ag [18-21], Pt [22,23], and FePt [24] embedded in silica matrix, to prolate shape. No shape deformation is observed for embedded Fe NPs in silica matrix by 120 MeV Au⁹⁺ ions at a fluence of 3×10^{13} ions/cm². However, tilt of easy axis of magnetization [25,26] was observed and explained by ion hammering effect. The deformation behavior of silica nanospheres, i.e., expansion in the direction perpendicular to ion beam and shrinkage in the direction parallel

* Correspondence: hsehgaj_007@yahoo.com

¹Nanotech Laboratory, Department of Physics, Indian Institute of Technology Delhi, New Delhi 110016, India.

Full list of author information is available at the end of the article

to ion beam, is known under the name “hammering effect” and explained by the viscoelastic thermal spike model [27,28]. On the other hand, there is no consistent theory describing the shape deformation of metal NPs in amorphous silica matrix, but the suggested mechanisms include melting of NPs in thermal spike [29-31], creep deformation induced by an overpressure due to differences in volume expansion and compressibility of NP and silica matrix [11], and shear stress-driven deformation due to in-plane strain perpendicular to ion beam direction [14,16,22,23].

In the present work, we report the elongation/anisotropic shape deformation of Ni NPs from spherical to prolate ones under 120 MeV Au⁺⁹ ion irradiation at fluence of 5×10^{13} ions/cm², where shape deformation strongly depends on the initial Ni particle size. Further, to understand the shape deformation process, simulations based on thermal spike model [29-31] were carried out and the effect of irradiation on structural and magnetic properties is presented.

Experimental details

A set of thin films of silica containing Ni NPs (Ni-SiO₂ nanogranular films) were synthesized by atom beam sputtering technique, as described elsewhere [32-35]. Silica and Ni were co-sputtered on thermally oxidized Si substrates mounted on a rotating sample holder. The relative area of silica and Ni chips exposed to the atom beam determines the concentration and size of Ni particles. In this study, the area of Ni was maintained to obtain ~10 at% Ni in the films. Ni-SiO₂ nanogranular films were annealed in Ar-H₂ (5%) atmosphere at 850°C (1 h) for promoting the growth of Ni particles and labeled as *pristine* film thereafter. The *pristine* film was irradiated at room temperature and at normal incidence with 120 MeV Au⁺⁹ ions at a fluence of 5×10^{13} ions/cm² in 15 UD Tandem Pelletron accelerator at the Inter University Accelerator Centre, New Delhi, India. The irradiation was performed in a high vacuum chamber with a base pressure of 2.8×10^{-6} Torr. The beam current was kept <0.5 pA (particle nano ampere) during irradiation to avoid heating of the film. The ion beam was uniformly scanned over 1×1 cm² area using an electromagnetic scanner. The range, electronic (S_e) and nuclear (S_n) stopping powers of 120 MeV Au⁺⁹ ions in silica were calculated using SRIM 2006 code [36] and amount to ~15 μ m, 14.7 keV/nm and 0.2 keV/nm, respectively. For such a large range, stopping powers can be considered constant over a film of few nanometers thickness. The composition and film thickness were measured by Rutherford backscattering spectrometry (RBS) using 1.7 MeV He⁺ ions at a scattering angle of 170°. Magnetization curves were measured using a Quantum Design MPMS SQUID magnetometer with a

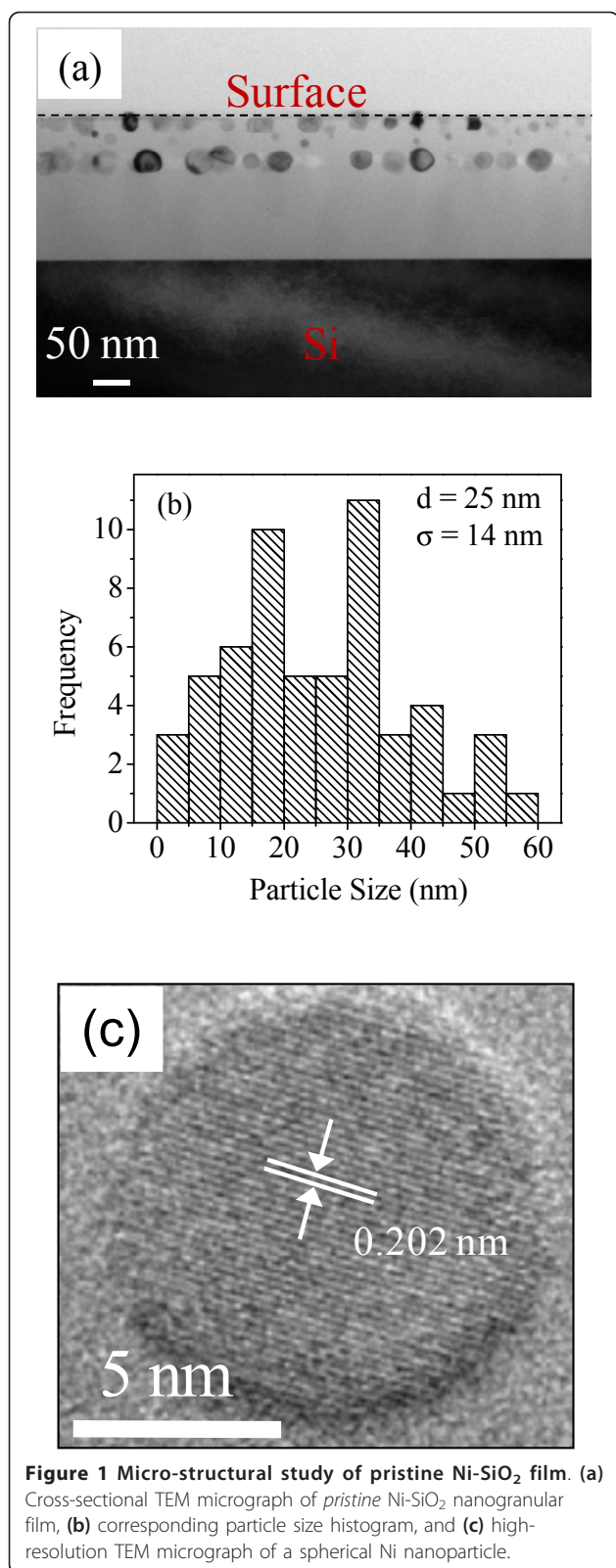
maximum field of 2 T applied parallel (out-plane measurement) and perpendicular (in-plane measurement) to the ion beam direction. TEM measurements were used to evaluate the size and shape evolution of Ni NPs before and after irradiation. TEM samples were prepared in cross-sectional geometry using the conventional techniques and were analyzed in FEI Titan 80-300 microscope working at accelerating voltage of 300 kV.

Results and discussion

The measured film thickness is ~150 nm with an average Ni atomic concentration of $10.5 \pm 1\%$ as estimated from fitting of RBS spectra using RUMP simulation code [37].

Micro-structural study

Figure 1a shows the cross-sectional TEM micrograph of *pristine* Ni-SiO₂ film and the corresponding histogram of particle sizes is shown in Figure 1b. It is clear from Figures 1a,b that the *pristine* film contains nearly spherical particles with a broad size distribution ranging from 3.8-60 nm with a mean particle size of ~25 nm. Figure 1c shows the high-resolution TEM micrograph of a particle evidencing its single crystalline nature and the measured lattice spacing of 0.202 nm corresponding to (111) plane of fcc Ni. Figure 2a shows the cross-sectional TEM micrograph of the *irradiated* film taking the direction of ion irradiation from top to bottom. It is clear from Figure 2a that most of the Ni NPs change from spherical to prolate shape with their major axis aligned along the direction of ion beam at a fluence of 5×10^{13} ions/cm². The elongated particles exhibit polycrystalline morphology, as apparent from high-resolution TEM micrograph (see Figure 2b). Figure 2c,d shows the histogram of major and minor axis length for prolate shape Ni particles. The mean major and minor axis lengths are 28.8 and 14.7 nm, respectively, estimated by considering all particles in Figure 2a. The mean aspect ratio for prolate-shaped particles is ~2. On comparing Figures 1a and 2a, it is observed that the smallest particles disappear after irradiation and shape deformation is completely suppressed for particles of size >14 nm. This confirms that the previous observations of shape deformation process is somewhat related to initial size of the nanoparticles, i.e., the bigger the particle the larger is its inertia against deformation/bigger particles require higher electronic stopping power for deformation [14-16]. Further, no deformation is observed for the free-standing Ni particles present at the surface of film (indicated by 1-3 in Figure 2a) and also those which are not surrounded by silica matrix completely (indicated by 4 in Figure 2a). This confirms previous observation by Pennikof *et al.* [38], which demonstrated the need of the surrounding matrix for shape deformation process upon



comparison with free-standing particles. SHI irradiation is known for modification of materials due to removal of atoms from the surface of a material. This process is called electronic sputtering as it is governed by electronic stopping power at higher energies. Generally, a higher sputtering yield is observed for insulators (particularly silica) than metals [39-42], and this may be responsible for the removal of silica surrounding the surface Ni NPs in the *irradiated* film. TEM results indicate the dissolution of Ni particles much smaller than ion track in silica matrix (of which diameter will be discussed later), whereas the growth and elongation of relatively bigger particles by 120 MeV Au⁺⁹ ions at a fluence of 5×10^{13} ions/cm² and also a threshold size (14 nm) exists above which no shape deformation occurs under the studied beam parameters.

Magnetic study

In order to observe the effect of irradiation on magnetic properties, magnetization curves were measured at 5 K in a magnetic field applied both parallel (out-plane measurement) and perpendicular (in-plane measurement) to the ion beam direction. The M-H curves for *pristine* and *irradiated* film are shown in Figure 3a, b, respectively. The extracted coercivity (H_c) and remanence ratio (M_r/M_s) from Figure 3a,b are given in Table 1. It is clear from Figure 3a that the *pristine* film has a small magnetic anisotropy with easy axis in the direction perpendicular to ion beam (in-plane). The origin of in-plane easy axis is the over-all thin film-like structure, i.e., anisotropy arising from the shape effect results in an in-plane easy axis, as similarly observed in case of Fe: SiO₂ granular films [25,26]. The other factors like magneto-crystalline, magnetostriction and shape anisotropy may be neglected as *pristine* film is polycrystalline in nature and without stress as confirmed by X-ray diffraction studies (figure not shown) containing spherical Ni particles (see Figure 1a). However, after 120 MeV Au⁺⁹ ion irradiation, the change in H_c and M_r/M_s values is much larger in the direction parallel to Au ion beam than in the perpendicular direction, which can be correlated with the elongation/formation of prolate shape Ni particles in the beam direction. Hence, magnetic shape anisotropy appears in the elongated Ni NPs with easy axis in the direction of elongation. However, a macroscopic magnetic anisotropy with easy axis in the ion beam direction is not observed due to the existence of some spherical Ni particles in addition to deformed prolate particles in the *irradiated* film.

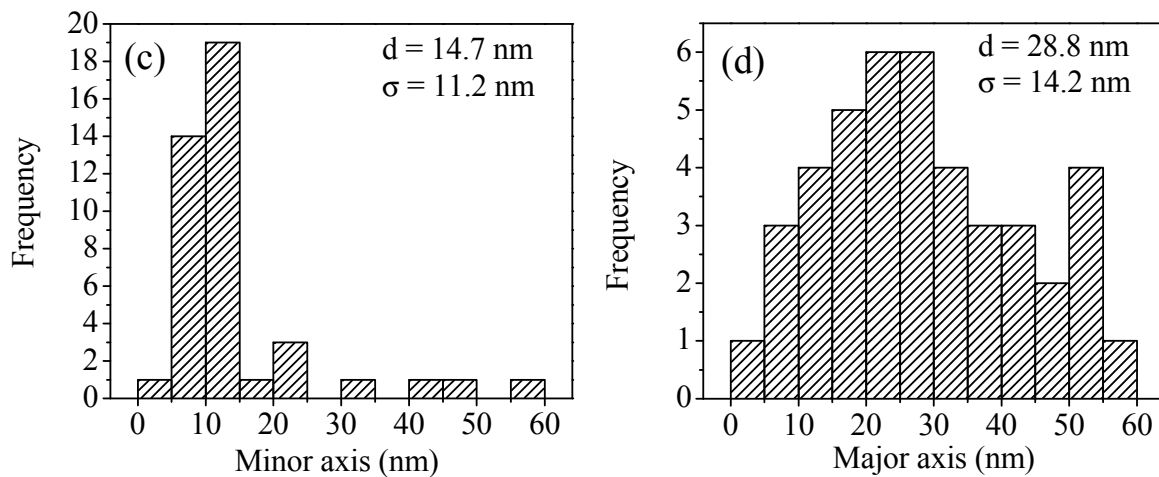
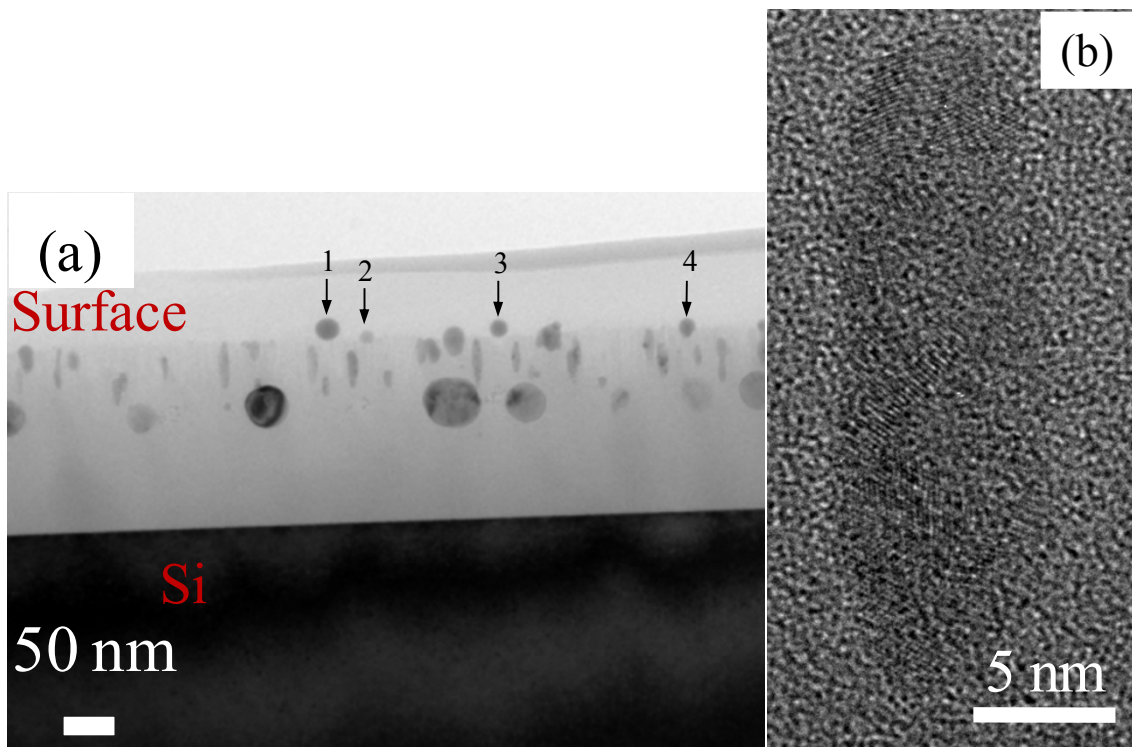


Figure 2 Micro-structural study of irradiated Ni-SiO₂ film. (a) Cross-sectional TEM micrograph of irradiated Ni-SiO₂ nanogranular film, (b) high-resolution TEM micrograph of an elongated Ni particle, and (c), (d) histogram of minor and major axis lengths of elongated particles, respectively.

Simulations based on thermal spike model

In order to elucidate the anisotropic shape deformation of Ni NPs under SHI irradiation, we adopt the thermal spike model to simulate the temperature evolution around the Ni NPs. Here, we extend the thermal spike

model to permit simulations for multiphase materials [14], considering the ion to pass through the center of Ni particle. In the thermal spike model [29-31], an incident heavy ion imparts its energy initially to target electrons and excites them to high temperature (within

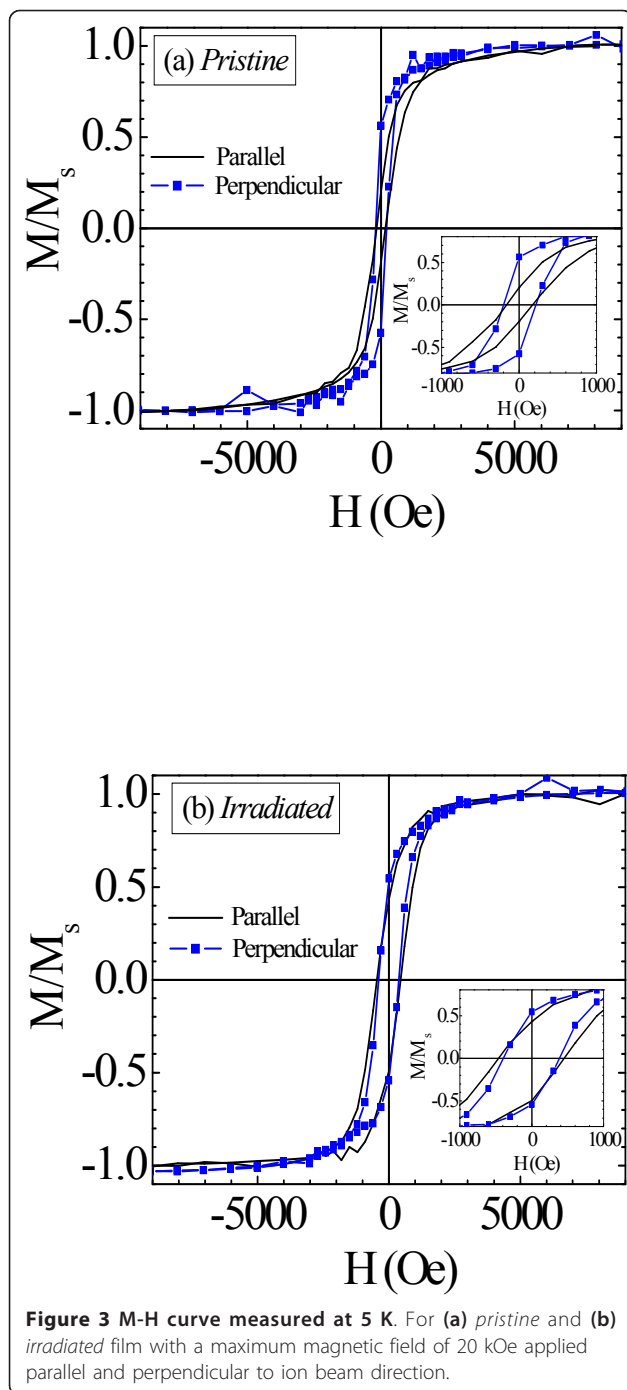


Figure 3 M-H curve measured at 5 K. For (a) *pristine* and (b) *irradiated* film with a maximum magnetic field of 20 kOe applied parallel and perpendicular to ion beam direction.

Table 1 Coercivity (H_c) and remanence ratio (M_r/M_s) measured at 5 K for the *pristine* and *irradiated* Ni-SiO₂ nanogranular film with magnetic field parallel and perpendicular to the 120 MeV Au⁺⁹ ion beam direction

Sample	Parallel		Perpendicular	
	H_c (Oe)	M_r/M_s	H_c (Oe)	M_r/M_s
<i>Pristine</i>	168	0.19	208	0.56
<i>Irradiated</i>	457	0.45	388	0.54

~1-10 fs) and is subsequently transferred from hot electrons to lattice vibrations through electron-electron scattering (within ~100 fs) and then electron-phonon coupling, causing an increase in lattice temperature above the melting point of the target within 0.1-10 ps depending upon the target under consideration. After ~0.1-1 ns the thermal spike cools down to ambient conditions. This process can be described by a set of coupled thermal diffusion equations [43] for electronic and lattice subsystems.

$$C_{ei}(T) \frac{\partial T_e}{\partial t} = \nabla[K_{ei}(T)\nabla T_e] + A(r, t) - g_i(T_e - T_l), \quad (1)$$

$$\rho_{li}C_{li}(T) \frac{\partial T_l}{\partial t} = \nabla[K_{li}(T)\nabla T_l] + g_i(T_e - T_l) \quad (2)$$

where T_e , T_l , $C_{ei}(T)$, $C_{li}(T)$, $K_{ei}(T)$ and $K_{li}(T)$ are the temperatures, the specific heats, and thermal conductivities of electronic (subscript e) and lattice (subscript l) subsystems, respectively; g_i is the electron-phonon coupling constant; ρ_{li} is the density of lattice, where $i = \text{Ni, SiO}_2$ represents the Ni particle region and surrounding SiO₂ region, respectively. $A(r, t)$ is the energy density per unit time transferred from incident ions to the electronic subsystem at a distance r and at time t from ion path. As according to the thermal spike model the lattice temperature for times ~1-10 ps is more like the representation of the energy transferred to the lattice. Therefore, radial distribution of lattice temperature is simulated within 1, 5, and 10 ps of 120 MeV Au⁺⁹ ion impact for Ni particles (2, 4, 6, 10, 15, 20, 30 nm) embedded in silica matrix. Table 2 shows the fitted values of the various parameters used for Ni [44] and silica [30,45] in the thermal spike model-based simulations.

Figure 4a shows, schematically, a simplified two-dimensional model, in which a 120 MeV Au⁺⁹ ion passes through the center of a spherical Ni particle embedded in silica matrix. Figure 4b,c shows the simulated radial distribution of the lattice temperature within 1 and 10 ps of 120 MeV Au⁺⁹ ion impact, for bulk silica and Ni nanoparticles (diameter, 2-30 nm) embedded in a silica matrix. It is well studied that a latent track may result due to the rapid quenching of the molten lattice. Here in our case, the estimated molten region in silica is ~10 nm from simulation results and agrees well with the earlier published experimental results [30]. Thermal spike simulations cannot be applied to surface NPs which behave differently (temperature evolution and stress relaxation) from embedded NPs. The following observations are evident from Figure 4b, c: (1) For $0 < d \leq 4$ nm Ni particles temperature reaches up to its bulk

Table 2 The fitted values of mass density (ρ), melting temperature (T_M), vaporization temperature (T_V), latent heat of fusion (L_M), latent heat of vaporization (L_V), lattice specific heat (C_l), lattice thermal conductivity (K_l) and electron-phonon coupling constant (g_l) for Ni and SiO₂ used in the thermal spike simulations [30,44,45]

Parameter	Ni	SiO ₂
ρ (g cm ⁻³)	8.9	2.62 (solid), 2.32 (liquid)
T_M (K)	1,726	1,950
T_V (K)	3,005	3,223
L_M (J g ⁻¹)	290.3	142
L_V (J g ⁻¹)	6,442	4,715
C_l (J g ⁻¹ K ⁻¹)	$0.39 + 1.9 \times 10^{-4}T - 3.3 \times 10^{-8}T^2 + 3.8 \times 10^{-11}T^3$; ($300 < T < T_M$), 0.62; ($T > T_M$).	$0.65 + 3.297 \times 10^{-4}T$; ($300 < T < T_M$), $1.3 - 3 \times 10^{-7}T$; ($T > T_M$).
K_l (WK ⁻¹ cm ⁻¹)	$3.4 - 1.3 \times 10^{-2}T + 2.12 \times 10^{-5}T^2 - 1.5 \times 10^{-8}T^3 + 3.6 \times 10^{-12}T^4$; ($100 < T < T_M$), 0.5 ($T > T_M$)	1×10^{-3} ($T > 300$)
g_l (W cm ⁻³ K ⁻¹)	9.54×10^{11}	1.25×10^{13}

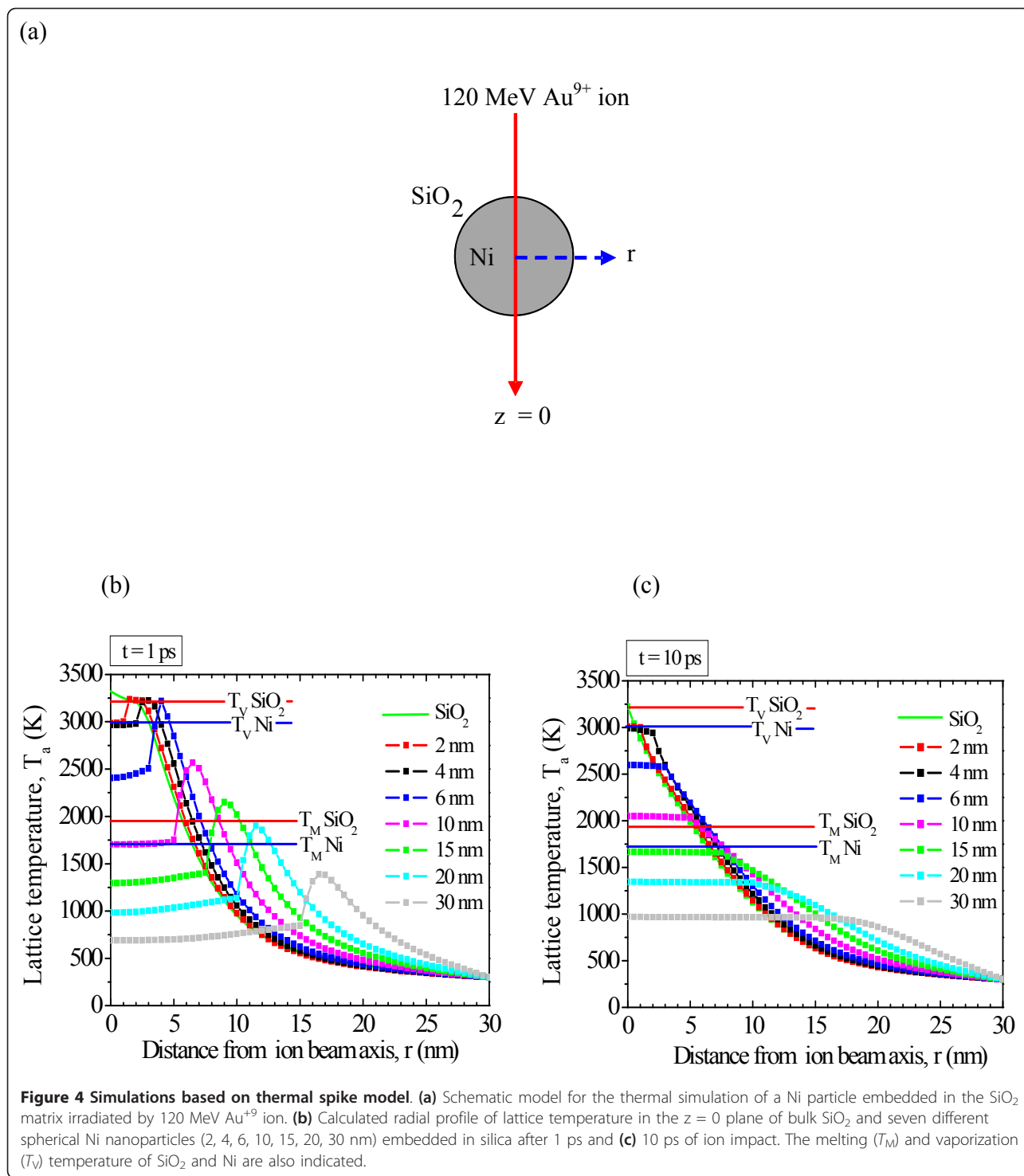
vaporization temperature (T_V) throughout its volume, so Ni atoms dissolve in the cylindrical molten silica track and promote the growth of neighboring bigger nanoparticles (>4 nm) by a ripening process, (2) For $4 < d \leq 10$ nm Ni particles, the lattice temperature of both Ni and surrounding silica rises above their respective melting points, so both Ni and silica are in molten state. Because of high electron-lattice coupling constant and low thermal conductivity of silica as compared to Ni, the temperature rise in silica is high as compared to metallic Ni even though incident ion energy is deposited to Ni and then coupled to silica, but thermal evolution itself does not give full explanation for deformation of metal NPs and hence shear stress also needs to be included as another factor in shape deformation. (3) For Ni particles having diameter >10 nm, Ni particle and surrounding silica both have temperature below their respective melting point and so retain their original shape. However, from TEM micrographs it is observed that Ni particles of size <14 nm are deformed and shape deformation is completely suppressed for particles of size >14 nm. The diameter in experiments does not match exactly with those obtained from thermal spike model-based simulations as pressure-dependent variation of thermodynamic parameters is neglected and size dependent variation of thermodynamic parameters is unknown, and hence the bulk values for Ni are used in the present case. The outcome of thermal spike simulations is that the lattice temperature of smaller size Ni particles increases much higher than lattice temperature of relatively bigger particles and experimental results are explainable within errors.

One may also think *ion hammering* as responsible mechanism for the elongation of Ni NPs. However, according to ion hammering mechanism, a large elongation is expected for smaller particles than relatively bigger particles, which contradicts our observation and hence rules out ion hammering effect. Klaumünzer *et al.*

[46] also pointed out that hammering as an indirect mechanism alone is not sufficient to account for the observed deformation of solid NPs, i.e., the metallic NP must actively participate in the deformation process. In other words, elongation occurs only when the lattice temperatures of both metallic NP and the dielectric SiO₂ exceed their respective individual melting temperatures, i.e., elongation of embedded NPs occur due to flow of metallic species into molten silica tracks [14,22]. According to the viscoelastic thermal spike model [27,28], the origin of anisotropic shape deformation of amorphous materials, e.g., silica is due to relaxation of shear stresses in the ion track region. These shear stresses are generated due to rapid thermal expansion of the ion-induced thermal spikes. The complete relaxation in the track region is assumed to take place when the ion track temperature exceeds a certain flow temperature (melting point). As for $4 < d \leq 10$ nm diameter Ni NPs this condition (melting of Ni as well as surrounding silica) is satisfied, so combination of stress effects in silica and thermal spike model gives a fairly good explanation for the elongation/shape deformation from spherical to prolate shape of Ni NPs.

Conclusions

In conclusion, we report the elongation of Ni NPs parallel to each other embedded in silica matrix by 120 MeV Au⁺⁹ ion irradiation at fluence of 5×10^{13} ions/cm² with mean aspect ratio of ~2. Shape deformation is observed for particles <14 nm and is suppressed for particles >14 nm under studied beam parameters. Irradiation leads to formation of surface Ni particles without silica matrix and also not deformed, expected due to large electronic sputtering yield of silica. Large changes in coercivity (H_c) and remanence ratio (M_r/M_s) are observed in the direction parallel to Au⁺⁹ ion beam than in the perpendicular direction, which is due to the elongation/formation of prolate shape Ni particles in the



beam direction. However, a macroscopic perpendicular magnetic anisotropy is not observed due to the existence of both spherical and deformed prolate shape Ni particles in the *irradiated* film. The experimental observations are well explained by thermal spike model-based

simulations. Fabrication of *pristine* films with particles of average size in the range from 5 to 20 nm in order to control the macroscopic magnetic anisotropy with easy axis in the ion beam direction could be set as future perspective of this work.

Acknowledgements

One of the authors (H. Kumar) acknowledges CSIR India for financial support as SRF and Dr. D. C. Agarwal (research associate, IUAC Delhi) for his kind help during sample preparation. One of the authors (D.K.A.) is thankful to Department of Science and Technology (DST), India for providing the financial assistance for 'Atom beam source' under the project 'Nanostructuring by energetic ion beams' under Nano-mission. We also acknowledge the Pelletron group, IUAC Delhi for providing stable beam during irradiation experiment.

Author details

¹Nanostech Laboratory, Department of Physics, Indian Institute of Technology Delhi, New Delhi 110016, India. ²Inter University Accelerator Centre, Aruna Asaf Ali Marg, New Delhi 110067, India. ³Institute of Ion Beam Physics and Materials Research, Forschungszentrum Dresden-Rossendorf, P.O. Box 510119, 01314 Dresden, Germany. ⁴Institut d'Electronique du Solide et des Systemes, 23 rue du Loess, BP 20 CR, 67037 Strasbourg Cedex 2, France.

Authors' contributions

HK, SG, DKA and DK designed the experiments. HK and SG performed the experiments related to sample preparation and ion irradiation, AM performed the TEM analysis, SZ and HS performed the magnetic analysis, JPS performed the Thermal spike simulations. HK wrote the manuscript. All authors discussed the results and commented on the manuscript.

Competing interests

The authors declare that they have no competing interests.

Received: 19 August 2010 Accepted: 18 February 2011

Published: 18 February 2011

References

- Gerardy JM, Ausloos M: Absorption spectrum of clusters of spheres from the general solution of Maxwell's equations. II. Optical properties of aggregated metal spheres. *Phys Rev B* 1982, **25**:4204.
- Battle X, Labarta A: Finite-size effects in fine particles: magnetic and transport properties. *J Phys D Appl Phys* 2002, **35**:R15.
- Murphy CJ, Gole AM, Hunyadi SE, Stone JW, Sisco PN, Alkilany A, Kinard BE, Hankins P: Chemical sensing and imaging with metallic nanorods. *Chem Comm* 2008, **5**:544.
- Lee KS, El-Sayed MA: Gold and silver nanoparticles in sensing and imaging: sensitivity of plasmon response to size, shape, and metal composition. *J Phys Chem B* 2006, **110**:19220.
- Dhawan A, Muth JF, Leonard DN, Gerhold MD, Gleeson J, Vo-Dinh T, Russell PE: Focused ion beam fabrication of metallic nanostructures on end faces of optical fibers for chemical sensing applications. *J Vac Sci Technol B* 2008, **26**:2168.
- Evans P, Hendren WR, Atkinson R, Wurtz GA, Dickson W, Zayats AV, Pollard RJ: Growth and properties of gold and nickel nanorods in thin film alumina. *Nanotechnology* 2006, **17**:5746.
- Chou SY, Wei MS, Krauss PR, Fischer P: Single-domain magnetic pillar array of 35 nm diameter and 65 Gbits/in.² density for ultrahigh density quantum magnetic storage. *J Appl Phys* 1994, **76**:6673.
- Huajun Z, Jinhuan Z, Zhenghai G, Wei W: Preparation and magnetic properties of Ni nanorod arrays. *J Magn Magn Mater* 2008, **320**:565.
- Snoeks E, van Blaaderen A, van Dillen T, van Kats CM, Brongersma ML, Polman A: Colloidal ellipsoids with continuously variable shape. *Adv Mater* 2000, **12**:1511.
- van Dillen T, Polman A, Fukarek W, van Blaaderen A: Energy-dependent anisotropic deformation of colloidal silica particles under MeV Au irradiation. *Appl Phys Lett* 2001, **78**:910.
- D'Orléans C, Stoquert JP, Estournès C, Cerruti C, Grob JJ, Guille JL, Haas F, Muller D, Richard-Plouet M: Anisotropy of Co nanoparticles induced by swift heavy ions. *Phys Rev B* 2003, **67**:220101R.
- D'Orléans C, Stoquert JP, Estournès C, Grob JJ, Muller D, Guille JL, Richard-Plouet M, Cerruti C, Haas F: Elongated Co nanoparticles induced by swift heavy ion irradiations. *Nucl Instrum Methods Phys Res B* 2004, **216**:372.
- Mishra YK, Singh F, Avasthi DK, Pivin JC, Malinowska D, Pippel E: Synthesis of elongated Au nanoparticles in silica matrix by ion irradiation. *Appl Phys Lett* 2007, **91**:063103.
- Awazu K, Wang X, Fujimaki M, Tominaga J, Aiba H, Ohki Y, Komatsubara T: Elongation of gold nanoparticles in silica glass by irradiation with swift heavy ions. *Phys Rev B* 2008, **78**:054102.
- Dawi EA, Rizza G, Mink MP, Vredenberg AM, Habraken FHPM: Ion beam shaping of Au nanoparticles in silica: Particle size and concentration dependence. *J Appl Phys* 2009, **105**:074305.
- Rizza G, Dawi EA, Vredenberg AM, Monnet I: Ion engineering of embedded nanostructures: From spherical to faceted nanoparticles. *Appl Phys Lett* 2009, **95**:043105.
- Rodríguez-Iglesias V, Peña-Rodríguez O, Silva-Pereyra HG, Rodríguez-Fernández L, Kellermann G, Cheang-Wong JC, Crespo-Sosa A, Oliver A: Elongated gold nanoparticles obtained by ion implantation in silica: Characterization and T-matrix simulations. *J Phys Chem C* 2010, **114**:746.
- Penninkhof JJ, Polman A, Sweatlock LA, Maier SA, Atwater HA, Vredenberg AM, Kooi BJ: Mega-electron-volt ion beam induced anisotropic plasmon resonance of silver nanocrystals in glass. *Appl Phys Lett* 2003, **83**:4137.
- Oliver A, Reyes-Esqueda JA, Cheang-Wong JC, Roman-Velazquez CE, Crespo-Sosa A, Rodríguez-Fernández L, Seman JA, Noguez C: Controlled anisotropic deformation of Ag nanoparticles by Si ion irradiation. *Phys Rev B* 2006, **74**:245425.
- Singh F, Mohapatra S, Stoquert JP, Avasthi DK, Pivin JC: Shape deformation of embedded metal nanoparticles by swift heavy ion irradiation. *Nucl Instrum Methods Phys Res B* 2009, **267**:936.
- Pivin JC, Singh F, Mishra YK, Avasthi DK, Stoquert JP: Synthesis of silica: Metals nanocomposites and modification of their structure by swift heavy ion irradiation. *Surf Coat Tech* 2009, **203**:2432.
- Giulian R, Kluth P, Araujo LL, Sprouster DJ, Byrne AP, Cookson DJ, Ridgway MC: Shape transformation of Pt nanoparticles induced by swift heavy-ion irradiation. *Phys Rev B* 2008, **78**:125413.
- Giulian R, Kluth P, Sprouster DJ, Araujo LL, Byrne AP, Ridgway MC: Swift heavy ion irradiation of Pt nanocrystals embedded in SiO₂. *Nucl Instrum Methods Phys Res B* 2008, **266**:3158.
- Pivin JC, Singh F, Angelov O, Vincent L: Perpendicular magnetization of FePt particles in silica induced by swift heavy ion irradiation. *J Phys D Appl Phys* 2009, **42**:025005.
- Singh F, Avasthi DK, Angelov O, Berthet P, Pivin JC: Changes in volume fraction and magnetostriction of iron nanoparticles in silica under swift heavy ion irradiation. *Nucl Instrum Methods Phys Res B* 2006, **245**:214.
- Pivin JC, Esnouf S, Singh F, Avasthi DK: Investigation of the precipitation kinetics and changes of magnetic anisotropy of iron particles in ion-irradiated silica gel films by means of electron-spin resonance. *J Appl Phys* 2005, **98**:023908.
- Trinkaus H, Ryazanov AI: Viscoelastic model for the plastic flow of amorphous solids under energetic ion bombardment. *Phys Rev Lett* 1995, **74**:5072.
- van Dillen T, Polman A, Onck PR, van der Giessen E: Anisotropic plastic deformation by viscous flow in ion tracks. *Phys Rev B* 2005, **71**:024103.
- Toulemonde M, Dufour C, Paumier E: Transient thermal process after a high-energy heavy-ion irradiation of amorphous metals and semiconductors. *Phys Rev B* 1992, **46**:14362.
- Meftah A, Brisard F, Costantini JM, Dooryhee E, Hage-Ali M, Hervieu M, Stoquert JP, Studer F, Toulemonde M: Track formation in SiO₂ quartz and the thermal-spike mechanism. *Phys Rev B* 1994, **49**:12457.
- Furuno S, Otsu H, Hojou K, Izui K: Tracks of high energy heavy ions in solids. *Nucl Instrum Methods Phys Res B* 1996, **107**:223.
- Kabiraj D, Abhilash SR, Vanmarcke L, Cinausero N, Pivin JC, Avasthi DK: Atom beam sputtering setup for growth of metal particles in silica. *Nucl Instrum Methods Phys Res B* 2006, **244**:100.
- Avasthi DK, Mishra YK, Kabiraj D, Lalla NP, Pivin JC: Synthesis of metal-polymer nanocomposite for optical applications. *Nanotechnology* 2007, **18**:125604.
- Mishra YK, Mohapatra S, Avasthi DK, Kabiraj D, Lalla NP, Pivin JC, Sharma H, Kar R, Singh N: Gold-silica nanocomposites for the detection of human ovarian cancer cells: a preliminary study. *Nanotechnology* 2007, **18**:345606.
- Kumar H, Ghosh S, Bürger D, Zhou S, Kabiraj D, Avasthi DK, Grötzschel R, Schmidt H: Microstructure, electrical, magnetic and extraordinary Hall

- effect studies in Ni: SiO₂ nanogranular films synthesized by atom beam sputtering. *J Appl Phys* 2010, **107**:113913.
36. Ziegler JF, Biersack ZP, Littmark U: **The stopping and range of ions in solids**. New York: Pergamon; 1985 [http://www.srim.org].
 37. Doolittle LR: **Algorithms for the rapid simulation of Rutherford backscattering spectra**. *Nucl Instrum Methods Phys Res B* 1985, **9**:344.
 38. Penninkhof JJ, van Dillen T, Roorda S, Graf C, van Blaaderen A, Vredenberg AM, Polman A: **Anisotropic deformation of colloidal metal-dielectric core-shell colloids under MeV ion irradiation**. *Nucl Instrum Methods Phys Res B* 2006, **242**:523.
 39. Toulemonde M, Assmann W, Trautmann C, Grüner F, Mieskes HD, Kucal H, Wang ZG: **Electronic sputtering of metals and insulators by swift heavy ions**. *Nucl Instrum Methods Phys Res B* 2003, **212**:346.
 40. Arnoldbik WM, van Emmichoven PAZ, Habraken FHPM: **Electronic sputtering of silicon suboxide films by swift heavy ions**. *Phys Rev Lett* 2005, **94**:245504.
 41. Mieskes HD, Assmann W, Grüner F, Kucal H, Wang ZG, Toulemonde M: **Electronic and nuclear thermal spike effects in sputtering of metals with energetic heavy ions**. *Phys Rev B* 2003, **67**:155414.
 42. Cheblukov Yu-N, Didyk A-Yu, Halil A, Semina VK, Stepanov AE, Suvorov AL, Vasiliev NA: **Sputtering of metals by heavy ions in the inelastic energy loss range**. *Vacuum* 2002, **66**:133.
 43. Lifshitz IM, Kaganov MI, Taratanov LV: **On the theory of radiation-induced changes in metals**. *J Nucl Energy Parts A* 1960, **12**:69.
 44. Wang ZG, Dufour Ch, Paumier E, Toulemonde M: **The S_e sensitivity of metals under swift-heavy-ion irradiation: a transient thermal process**. *J Phys Cond Mat* 1994, **6**:6733.
 45. Toulemonde M, Paumier E, Costantini JM, Dufour C, Meftah A, Studer F: **Track creation in SiO₂ and BaFe₁₂O₁₉ by swift heavy ions: a thermal spike description**. *Nucl Instrum Methods Phys Res B* 1996, **116**:37.
 46. Klaumünzer S: **Modification of nanostructures by high-energy ion beams**. *Nucl Instrum Methods Phys Res B* 2006, **244**:1.

doi:10.1186/1556-276X-6-155

Cite this article as: Kumar et al.: Ion beam-induced shaping of Ni nanoparticles embedded in a silica matrix: from spherical to prolate shape. *Nanoscale Research Letters* 2011 **6**:155.

Submit your manuscript to a SpringerOpen[®] journal and benefit from:

- Convenient online submission
- Rigorous peer review
- Immediate publication on acceptance
- Open access: articles freely available online
- High visibility within the field
- Retaining the copyright to your article

Submit your next manuscript at ► springeropen.com
